Since January 2020 Elsevier has created a COVID-19 resource centre with free information in English and Mandarin on the novel coronavirus COVID-19. The COVID-19 resource centre is hosted on Elsevier Connect, the company's public news and information website.

ACADEMIC PRESS

Available online at www.sciencedirect.com

SCIENCE DIRECT®

VIROLOGY

Virology 311 (2003) 16–27

www.elsevier.com/locate/yviro

Emergence of a coronavirus infectious bronchitis virus mutant with a truncated 3b gene: functional characterization of the 3b protein in pathogenesis and replication

S. Shen,[a] Z.L. Wen,[a] and D.X. Liu[b,*]

[a] *Institute of Molecular and Cell Biology, National University of Singapore, Singapore 117604*

[b] *School of Biological Sciences, Nanyang Technological University, 1 Nanyang Walk, Block 5, Level 3, Singapore 637616*

Received 4 September 2002; returned to author for revision 29 October 2002; accepted 20 December 2002

Abstract

The subgenomic RNA 3 of IBV has been shown to be a tricistronic mRNA, encoding three products in IBV-infected cells. To explore if the least expressed ORF, ORF 3b, which encodes a nonstructural protein, is evolutionarily conserved and functionally indispensable for viral propagation in cultured cells, the Beaudette strain of IBV was propagated in chicken embryonated eggs for three passages and then adapted to a monkey kidney cell line, Vero. The 3b gene of passage 3 in embryonated eggs and passages 7, 15, 20, 25, 30, 35 50, and 65 in Vero cells were amplified by reverse transcription–polymerase chain reaction and sequenced. The results showed that viral RNA extracted from passages 35, 50, and 65 contained a single A insertion in a 6A stretch of the 3b gene between nucleotides 24075 and 24080, whereas the early passages carried the normal 3b gene. This insertion resulted in a frameshift event and therefore, if expressed, a C-terminally truncated protein. We showed that the frameshifting product, cloned in a plasmid, was expressed in vitro and in cells transfected with the mutant construct. The normal product of the 3b gene is 64 amino acids long, whereas the frameshifting product is 34 amino acids long with only 17 homogeneous amino acid residues at the N-terminal half. Immunofluorescent studies revealed that the normal 3b protein was localized to the nucleus and the truncated product showed a "free" distribution pattern, indicating that the C-terminal portion of 3b was responsible for its nuclear localization. Comparison of the complete genome sequences (27.6 kb) of isolates p20c22 and p36c12 (from passages 20 and 36, respectively) revealed that p36c12 contains three amino acid substitutions, two in the 195-kDa protein (encoded by gene 1) and one in the S protein, in addition to the frameshifting 3b product. Further characterization of the two isolates demonstrated that p36c12 showed growth advantage over p20c22 in both Vero cells and chicken embryos and was more virulent in chicken embryos than p20c22. These results suggest that the 3b gene product is not essential for the replication of IBV.

Introduction

Avian coronavirus infectious bronchitis virus (IBV) is a member of the Coronaviridae family in the new order Nidovirales (Cavanagh et al., 1997). Coronavirus itself is further divided into three groups on the basis of the antigenicity, genome organization, and sequence homology (Enjuanes et al., 1998, 2000). IBV, together with turkey coronaviruses (TCoV) and pheasant coronaviruses (PhCoV), belongs to group III (Cavanagh, 2001a; Cavanagh et al., 2001b, 2002; Guy, 2000). It is an enveloped virus with a single positive-stranded RNA genome of 27.6 kb in length. Upon virus entry into cells, a 3′-coterminal nested set of six mRNAs is produced. About 74% of the genome at the 5′-end comprises two overlapping replicase genes, expressing from the genomic RNA or mRNA 1 in the form of polyproteins 1a and 1a/b. The polyproteins are subsequently processed into at least 10 nonstructural proteins by virus-encoded proteinases (Lim et al., 2000; Ng et al., 2000; Xu et al., 2001). These mature and intermediate products are involved in the genomic and subgenomic (sg) RNA synthesis. The four structural proteins, spike (S), envelope (E), membrane (M), and nucleocapsid (N), are encoded by sgRNAs 2, 3, 4, and 6, respectively. Meanwhile, four small nonstructural proteins, 3a, 3b, 5a, and 5b, are also encoded

* Corresponding author. Fax: +65-68968032.
E-mail address: dxliu@ntu.edu.sg (D.X. Liu).

0042-6822/03/$ – see front matter © 2003 Elsevier Science (USA). All rights reserved.
doi:10.1016/S0042-6822(03)00117-X

by sgRNAs 3 and 5. The functions of the structural proteins S, E, M, and N have been extensively studied, whereas little is known about the functions of the nonstructural 3a, 3b, 5a, and 5b. Similar small ORFs, interspersed among the structural genes S, E, M, and N, are also found in other coronaviruses. For example, two to five ORFs for nonstructural proteins were found in group I coronaviruses, and three to four ORFs for nonstructural proteins and two for minor structural proteins, hemoagglutinin esterase (HE) and internal gene product (I) of the N gene, were identified in group II coronaviruses. The identities and locations of these group-specific genes vary among different viruses. These structural and nonstructural genes are referred to as accessory genes, as they might be dispensable for viral replication (De Vries et al., 1997). Strains lacking one of these genes are still viable at least in vitro and sometimes in vivo.

In general for coronaviruses, only the 5′-ORF of each sgRNA is translated. However, the second and even the third ORF of several sgRNAs are translated by mechanisms of internal initiation or leaky ribosomal scanning (Liu and Inglis, 1991b; Senanayake et al., 1992; Thiel and Siddell, 1994). These include the 3b, 3c (for E), and 5b from sgRNAs 3 and 5 of IBV; the 5b (for E) from sgRNA 5 of murine hepatitis virus (MHV); and the 3b, 3c, and 7b from sgRNAs 3 and 7 of canine coronavirus, respectively (Horsburgh et al., 1992; Liu et al., 1991a; Liu and Inglis, 1991b, 1992a; Yu et al., 1994). One of the distinguishing features of group III coronaviruses is that the third ORF 3c of the tricistronic mRNA 3 encodes the E protein, which, together with the M protein, plays an essential role in virus particle assembly (Bos et al., 1996; Vennema et al., 1996).

The 3a, 3b, 5a, and 5b proteins of IBV have been identified in virus-infected cells (Liu and Inglis, 1991a, 1992a), but their roles in the IBV life cycle are still unknown. High sequence identity between these genes in IBV, TCoV, and PhCoV is observed (Cavanagh et al., 2001b, 2002), but sequence similarities are very low, if any, when compared with the nonstructural, accessory genes of group I and II coronaviruses. It seems that these genes are unique for group III coronaviruses of birds (Cavanagh et al., 2001b, 2002; Guy, 2000), like the HE and 2a genes found only in group II viruses (Bredenbeek et al., 1990) and the homologous accessory genes among group I viruses (Enjuanes et al., 2000). It has been reported that genes 2a, 4, and 5a, encoding nonstructural proteins (Luytjes et al., 1988; Ontiveros et al., 2001; Schwarz et al., 1990; Weiss et al., 1993; Yokomori and Lai, 1991b), and the two structural genes HE and I (Fischer et al., 1997; Yokomori et al., 1991a) of MHV are nonessential for virus replication in cultured cells. Some of these accessory genes might be related to host specificity, cell tropism, and pathogenesis (Herrewegh et al., 1995; Wesley et al., 1990; de Haan et al., 2002). However, in most cases, the effects of these gene products on animal hosts and the reasons that these ORFs have been maintained throughout evolution are yet to be understood.

Here we present a report of isolation of an IBV strain with an abnormal 3b gene encoding a C-terminally truncated product. This was due to a single base insertion at the 5′-terminal portion of the 3b gene, leading to frameshift and a product with only 17 homogeneous amino acid residues. Interestingly, the mutant emerged after IBV was adapted from chicken embryos to Vero cells, a monkey kidney cell line. During passage of the virus in Vero cells, the mutant showed growth advantage over wild-type virus and became a dominant strain quickly. The growth abilities of two isolates, p20c22 and p36c12, carrying a normal and a truncated 3b gene, respectively, were characterized in both Vero cells and embryonated eggs. The results indicated that p36c12 propagated more quickly and produced larger plaques than p20c22 in Vero cells and might be more virulent in chicken embryos. The normal 3b protein was localized to the nucleus, whereas the truncated form showed a defuse distribution pattern. To our knowledge, this is the first coronavirus nonessential, nonstructural protein shown to be localized to the nucleus.

Results

The Beaudette strain of IBV was propagated in embryonated eggs 3 times and then adapted to Vero cells. The complete genome nucleotide sequence of a plaque-purified isolate, wt6501, from the passage 65 was determined and compared with those of other IBV strains, including the Beaudette strain (Boursnell et al., 1987) (GenBank: M95169). The results showed that a single base was inserted in a 6A stretch (Fig. 1a) between nucleotides 24075 and 24080, among mutations and deletions at other positions in the genome (Shen and Liu, unpublished observations). This insertion is located at the 5′-terminal region of the 3b gene, causing a frameshift and therefore resulting in a C-terminally truncated product if synthesized. The truncated product would contain 17 identical residues at the N-terminal half and 17 different residues at the C-terminal half, instead of 64 residues for the normal 3b protein (Fig. 1b).

Occurrence of the mutation in the 3b gene after adaptation of the virus to Vero cells

To investigate whether the insertion occurred after the virus was switched to a new host, sequence analysis of earlier passages was carried out. The passage 3 (EP3) in embryonated eggs and passages 7, 15, 20, 25, 30, 35, and 50 (p7 to p50) in Vero cells were chosen for reverse transcription–polymerase chain reaction (RT–PCR) amplification and sequence analysis of the 3b gene. The sequence profiles of RT–PCR products would represent the populations of the viral RNAs presented in a given passage. Overlapping peaks at the same position, representing different populations of viral RNAs, would be observed if wild-type and mutant viruses coexisted. As shown in Fig. 2, a single A insertion was detected in viral RNA prepared from p50, and two

a

```
3b  ATGTTAAACT TAGAAGTAAT TATTGAAACT GGTGAGCAAG TGATTCAAAA AATCAGTTTC
3B  ATGTTAAACT TAGAAGTAAT TATTGAAACT GGTGAGCAAG TGATTC[AAAAAAA]TCAGTTTC

    AATTTACAGC ATATTTCAAG TGTATTAAAC ACAGAAGTAT TTGATCCCTT TGACTATTGT
    AATTTACAGC ATATTTCAAG TGTATTAAAC ACAGAAGTAT TTGATCCCTT TGACTATTGT

    TATTACAGAG GAGGTAATTT TTGGGAAATA GAGTCAGCTG AAGATTGTTC AGGTGATGAT
    TATTACAGAG GAGGTAATTT TTGGGAAATA GAGTCAGCTG AAGATTGTTC AGGTGATGAT

    GAATTTATTG AATAA
    GAATTTATTG AATAA
```

b

```
3b  MLNLEVIIETGEQVIQKISFNLQHISSVLNTEVFDPFDYCYYRGGNFWEIESAEDCSGDDEFIE.
3B  MLNLEVIIETGEQVIQKNQFQFTAYFKCIKHRSI.SL.LLLLQRR.FLGNRVS.RLFR...IY.I
```

Fig. 1. Comparison of the nucleotide (a) and amino acid (b) sequences of the 3b gene between wt virus and the mutant. The site where an extra A was inserted in a 6A stretch and the predicted frameshift product with only 17 homogeneous amino acid residues are shown in bold. The resulting termination codons in the mutant 3B gene are underlined.

overlapping peaks representing an A and a T were observed at the same position in viral RNA prepared from p30 (Fig. 2A). Systematic sequence analysis of other passages demonstrated that the insertion was detected in p25, confirming that the insertion had occurred after the virus had been adapted to a new host. The mutant prevailed quickly in the population in less than 25 passages, suggesting that the mutant may have a growth advantage over wild-type virus.

Furthermore, 10 independent plaques were picked from each of passages 20 and 36, and the 3b gene of each isolate was sequenced. Sequence analysis revealed that 1 of 10 isolates from passage 20 carried the single A insertion (a 7A

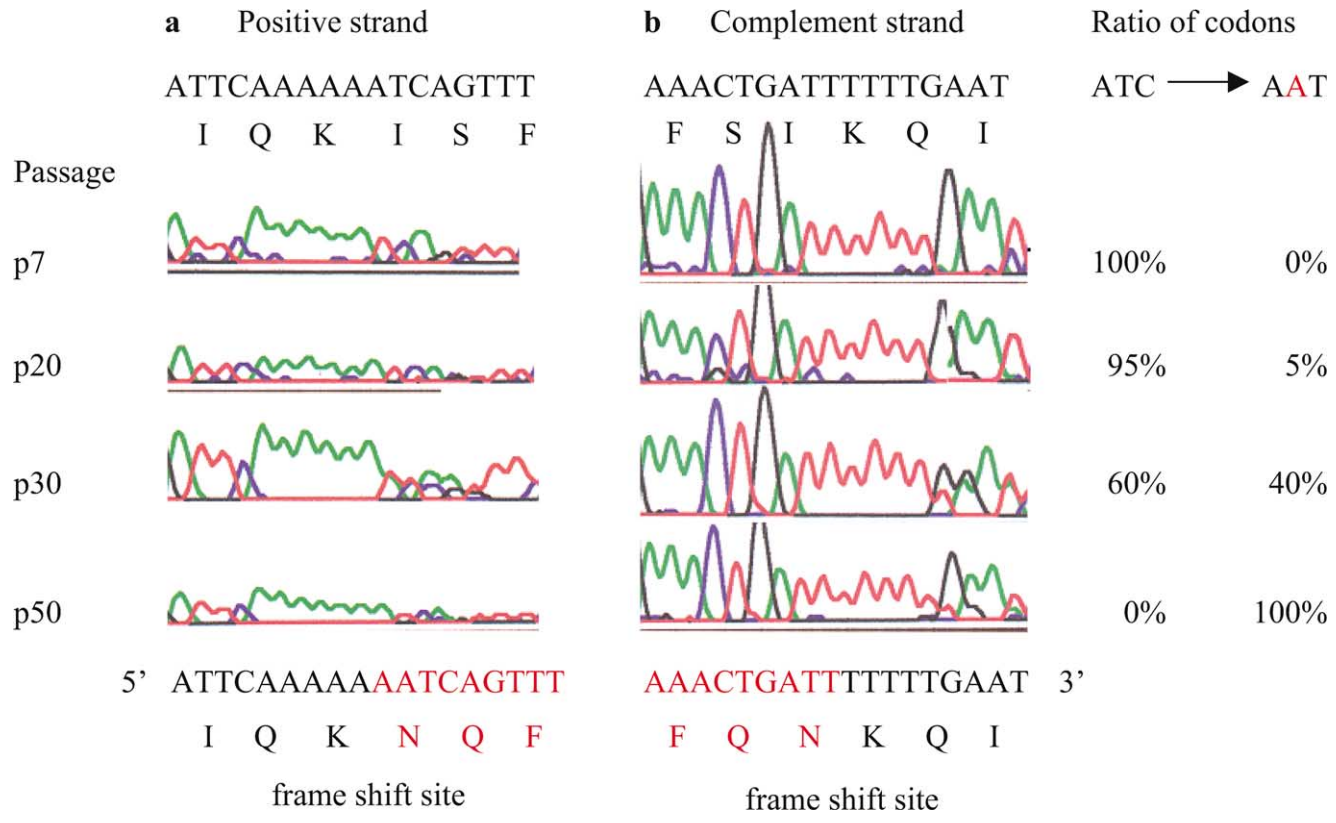

Fig. 2. The emergence of a 3′-end truncated 3b gene by insertion of a single nucleotide (A) during passage of IBV in Vero cells. The nucleotide sequences flanked the insertion site of both positive and complementary strands of passages 7, 20, 30, and 50 are shown. The percentage of the RNA population with the insertion in a given passage was estimated and indicated on the right, and the nucleotide and amino acid sequences of the normal and mutant 3b gene are indicated on the top and the bottom, respectively. The codons for the heterogeneous amino acid residues of the mutant 3B gene are indicated in red.

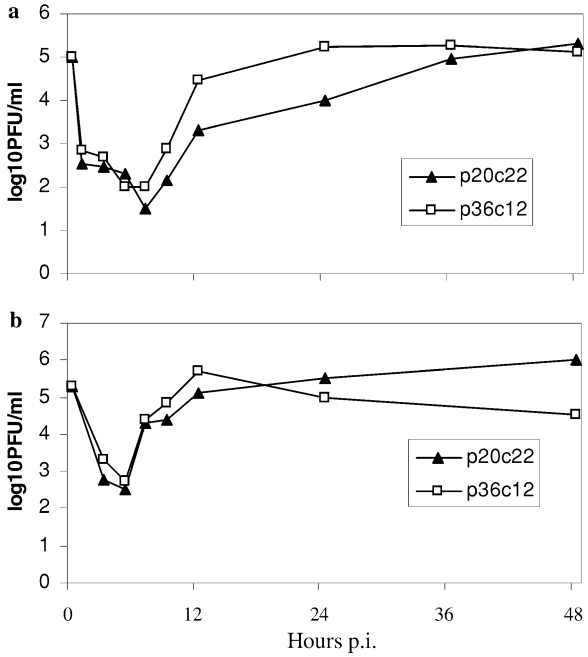

Fig. 3. Growth curves of p20c22 and p36c12 in Vero cells (a) and in chicken embryos (b). Vero cells were infected with p20c22 and p36c12, respectively, at a m.o.i. of 0.1 and embryonated eggs were inoculated with 4×10^4 PFU of either virus in 0.2 ml medium. Samples were collected from the infected cells or allantoic fluids and titrated on Vero cells. The experiments were independently repeated twice and each titration contained three duplicates.

stretch). By contrast, only 1 of 10 isolates from passage 36 contained the normal 6A stretch. These results indicated that viruses with the single A insertion dominated quickly during passage and had growth advantage over wild-type virus in both Vero cells and embryonated eggs

To understand why the mutant became dominant so quickly and viruses with a normal 3b gene was almost undetectable within less than 25 passages, the growth properties of two viruses in Vero cells and in embryonated eggs were examined. Two viruses, p20c22 (without the single A insertion) and p36c12 (with the insertion), were plaque-purified from passages 20 and 36, respectively, and the genotypes of the two viruses were confirmed by sequencing the RT–PCR fragments from both directions. To compare the growth abilities of the two viruses in Vero cells, same amounts of each virus (2×10^5 PFU/dish) were added to the cells in 35-mm dishes (at a m.o.i. of $\sim$0.1). Samples were collected at 0, 1, 3, 5, 7, 9, 12, 24, 36, and 48 h postinfection (p.i.), and the titers of virus in each sample were determined by plague assays on Vero cells. The growth curves of the two viruses in Vero cells are shown in Fig. 3a. Clearly from 7 to 24 h p.i., the titer of p36c12 was about 2 to 10 times as high as that of p20c22. P36c12 reached its peak at 24 h p.i., whereas p20c22 was 24 h later at 48 h p.i. The experiment was repeated twice. The gradual decrease of the titers of p36c12 observed from 36 to 48 h p.i. was likely due to the fact that p36c12 induced lysis of all infected cells much earlier than p20c22. Meanwhile, the plaque size of p36c12 was clearly bigger than that of p20c22, 2.2 mm vs 1.1 mm ($\pm$ 0.2 mm) in diameter (Fig. 4). It was also observed that the cytopathic effect (CPE) induced by p20c22 was delayed about 12 to 24 h compared to p36c12. These results confirm that p36c12 exhibits growth advantage over p20c22 in Vero cells.

To test the growth properties of the two viruses in embryonated eggs, 0.2 ml of virus stock containing 4×10^4 PFU of viruses was injected into the allantoic cavity of 10-day-old embryonated egg each. The allantoic fluid from 3 eggs from each group was collected at different time points. Plaque assays were performed using supernatants of the centrifuged fluid to determine the virus titers of each sample. As shown in Fig. 3b, the titers of p36c12 at 9 and 12 h postinoculation were higher than those of p20c22. Afterwards, the titers of p36c12 dropped more quickly than those of p20c22. The decrease of the titers of p36c12 was likely due to the death of infected embryos, mimicking the situation in Vero cells. In fact, it was found that chicken embryos infected with p36c12 were dying at 12 h postinfection, at least 12 h earlier than those infected with p20c22 when 4×10^4 PFU per egg was used. These results demonstrated that the mutant IBV virus replicates well in the original host cells.

Sequence analysis of p20c22, p36c12, and EP3

After characterization of the growth ability of the two isolates, we decided to determine the complete sequences of p20c22, p36c12, and EP3 to see whether any other mutations occurred that could contribute to the phenotype. The mutations that cause amino acid changes are listed in Table

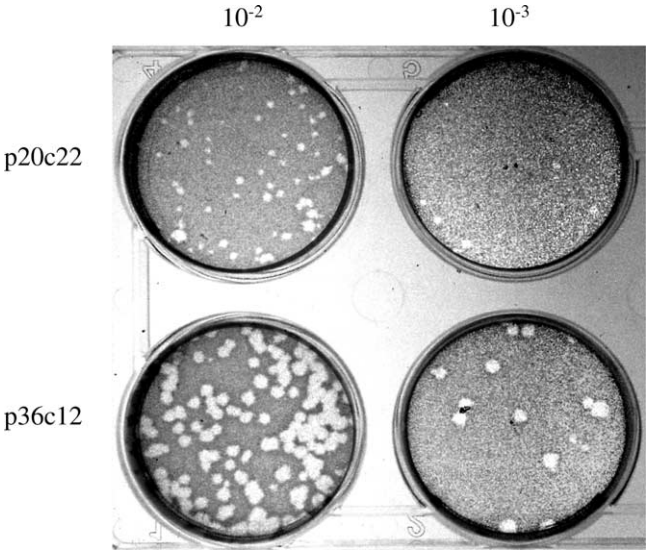

Fig. 4. Plaque sizes of p20c22 and p36c12. The viruses in passages 20 and 36 were plaque-purified three times, and the plaque sizes were compared after the genotypes were confirmed.

Table 1
Nucleotide (Nt) and amino acid (Aa) substitutions (in bold) of p20c22 and p36c12 compared to parental isolate EP3

Position	EP3		p20c22		p36c12	
	Nt	Aa	Nt	Aa	Nt	Aa
195kDa						
3283	A	K	G	E	G	E
3371	A	D	G	G	G	G
3926	T	L	T	L	C	S
4690	C	P	T	S	C	P
10kDa						
12332	A	D	G	G	G	G
39kDa						
18769	T	I	C	T	C	T
19189	C	P	T	L	T	L
S						
22609	A	T	G	A	G	A
22674(769)	A	I	A	I	G	M
22844	A	N	G	S	G	S
22938	A	L	T	F	T	F
23272	T	S	G	A	G	A
23402	G	S	T	L	T	L
3b						
24075/80	6A	QKI	6A	QKI	7A	QKN[a]
3c(E)						
24420	C	L	A	I	A	I

[a] The amino acid residue I is changed to an N as the result of frame-shifting.

1. Compared to EP3, 14 point mutations caused amino acid substitutions in three cleavage proteins of the 1a and 1a/b polyproteins and the S and E protein. However, only three substitutions were identified between p20c22 and p36c12, two in the 195-kDa protein and one in the S protein (I^{769}-M^{769}), in addition to the mutant 3b product of p36c12. Among the three isolates (EP3, p20c22, and p36c12), all amino acid substitutions in the spike protein occurred in the S2 region. As the S2 is more likely to be involved in membrane fusion rather than in receptor binding (Cavanagh et al., 1986; Saeki et al., 1997, Taguchi, 1995), it would be of interest to test the fusion activity of the S protein isolated from p20c22 and p36c12.

No difference in inducing membrane fusion by the S protein of both wild-type and mutant viruses

To investigate whether the I^{769}-M^{769} mutation was responsible for the growth and plaque-size phenotypes, we tested the membrane-fusion activity of the two constructs, pIBV-S20 and pIBV-S36, containing the S gene cloned from p20c22 and p36c12, respectively, by overexpression in Vero cells using the recombinant vaccinia/T7 virus system. As shown in Fig. 5, at 48 h posttransfection, the formation of massive syncytia was observed in cells expressing both pIBV-S20 and pIBV-S36, suggesting that the I^{769}-M^{769} mutation does not affect the membrane fusion activity of the S protein.

No inhibitory effect on the translatability of the mutant 3b gene and expression of the downstream E protein by the single A insertion

Next we investigated whether the predicted, C-terminally truncated 3b protein (3B) could be produced and whether the elongated poly-A stretch could affect the expression efficiency of the 3a and 3c genes. The 3c gene encodes the envelope protein, which plays an important role in budding and assembly of virion (Bos et al., 1996; Liu and Inglis, 1991b; Vennema et al., 1996). Plasmids (Fig. 6a) containing either wild-type 3b (3abc and 3bc) or the mutated 3B (3aBc and 3Bc) were constructed. in vitro transcription was carried out using T7 RNA polymerase and the yields of transcripts were quantified so that equal mole of RNAs from the paired plasmids, pIBV3abc/pIBV3aBc and pIBV3bc/pIBV3Bc,

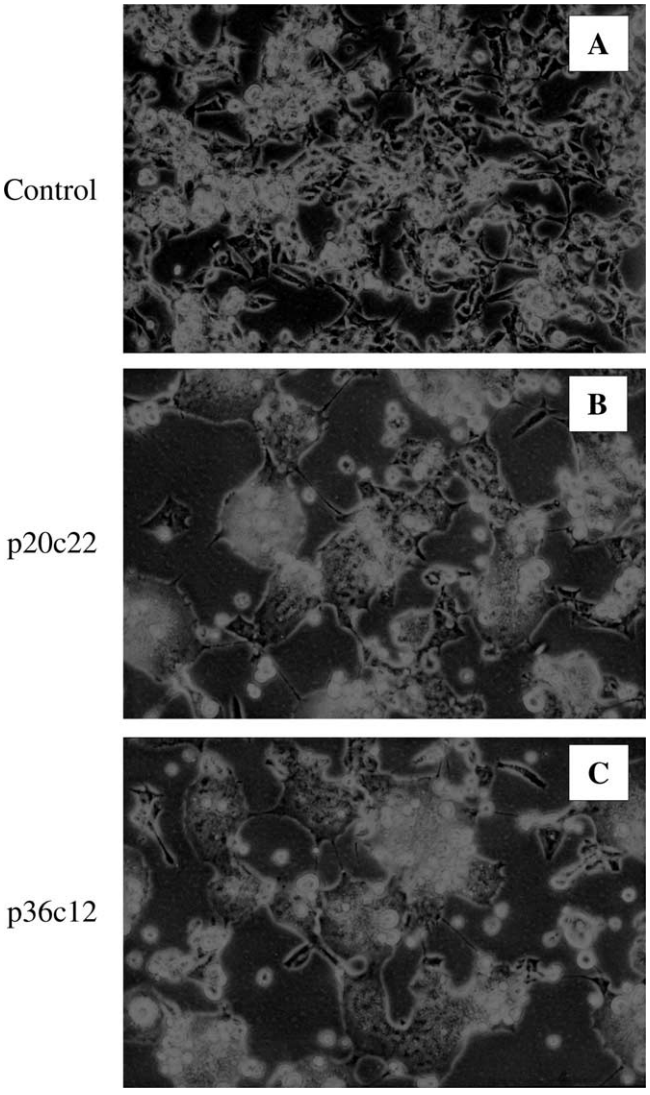

Fig. 5. Membrane fusion activity of the S gene. Plasmids containing the S protein derived from p20c22 (B) and p36c12 (C) were expressed in Vero cells using the T7/vaccinia expression system. The fusion activities were observed 2 days posttransfection.

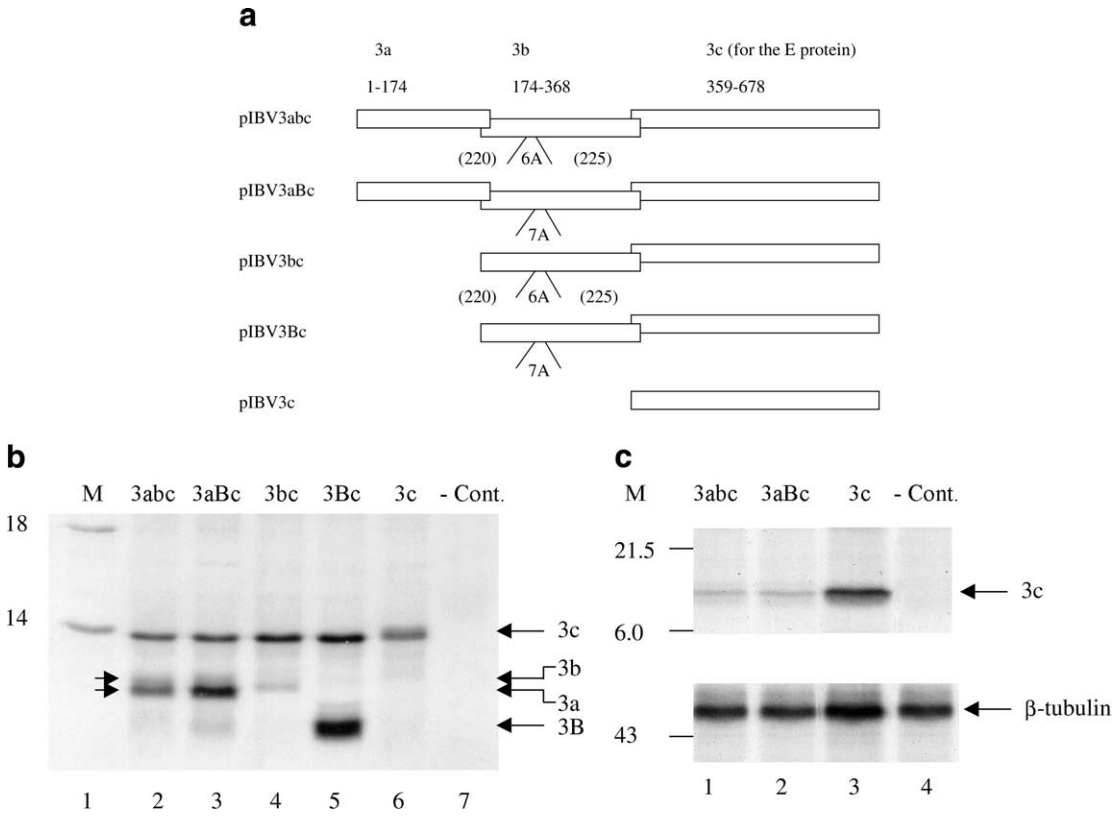

Fig. 6. (a) Diagram of constructs used for in vitro expression of the normal 3b and mutant 3B gene. Plasmids pIBV3abc, pIBV3bc, and pIBV3c were constructed with PCR fragments derived from passage 20, and pIBV3aBc and pIBV3Bc were constructed with PCR fragments from passage 36. The nucleotide positions of ORF3a, 3b, and 3c; the six A stretch; and the single A insertion site are indicated. (b) in vitro translation of constructs containing the normal 3b and mutant 3B gene. Equal amounts of RNA derived from pIBV3abc and pIBV3aBc or pIBV3bc and pIBV3Bc were used for in vitro translation in wheat germ lysates. RNA derived from pIBV3c was included as a positive control and water was added as a negative control. Numbers on the left indicate molecular masses in kilodaltons. (c) Expression of constructs containing the normal 3b and mutant 3B gene in intact cells. Equal amounts of plasmid DNA from pIBV3abc and pIBV3aBc were used for in vivo translation in Vero cells using the vaccinia/T7 expression system. Plasmid pIBV3c was included as a positive control and water was added as a negative control. Anti-β-tubulin antibody was used in immunoprecipitation as loading controls. Numbers on the left indicate molecular masses in kilodaltons.

could be used for the in vitro translation. As shown in Fig. 6b, the presence of the extra A in the 3B did not affect the 3c expression (lanes 2 and 3 and lanes 4 and 5), though the yield of the 3a protein from the construct pIBV3aBc was slightly increased (lanes 2 and 3). It was not surprising that a truncated, frameshifting product of about 3 kDa was observed (lanes 3 and 5) that was only expressed from constructs containing the 3B, but not the 3b gene. Plasmid pIBV3c containing only the 3c gene was included as a control and a marker (lane 6) for the expression of 3a, 3b, and 3c.

The effect of the insertion on translation of the 3c protein was further investigated by transfection of the same plasmids into Vero cells using vaccinia/T7 expression system. The results are shown in Fig. 6c. The 3c protein was immunoprecipitated with anti-E serum, and anti-β-tubulin antibody was used in immunoprecipitation as loading controls. As can be seen, similar levels of the 3c expression were observed when the 3abc construct was compared to the 3aBc construct (Fig. 6c, lanes 1 and 2). These results confirmed that the insertion does not affect the 3c protein expression in intact cells.

Induction of earlier death of chicken embryos by the more virulent mutant virus

To investigate the effect of the mutations on the pathogenesis of IBV, a same dosage (100 PFU/egg) of each virus was used to inoculate 10-day-old embryonated eggs. The infected embryos were incubated at 37°C and eight embryos from each group were sacrificed every 12 h postinoculation. Based on their movement and the extent of bleeding, curling, and dwarfing, the ratio of dead and alive embryos was determined. As shown in Table 2, 100% of embryos infected with p20c22 survived at 24 h postinoculation compared to only 50% of those with p36c12 ($P < 0.01$). At 36 h postinoculation, 75 and 100% of embryos infected with p20c22 and p36c12, respectively, were dead ($P < 0.05$). The experiment was repeated four times and similar results were obtained, suggesting that p36c12 is more virulent than

Table 2
Number of dead/total embryos inoculated with p20c22 and p36c12[a]

	12	24	36	48	72 (h)
Control	0/8	0/8	0/8	0/8	0/8
p20c22	0/8	0/8	6/8	8/8	8/8
p36c12	0/8	4/8	8/8	8/8	8/8

[a] The difference in the ratio of dead/total embryos infected with wild-type and mutant viruses at 24 and 36 h postinoculation, respectively, was analyzed by the paired *t* test (see text).

p20c22 in chicken embryos. This is consistent with the growth-curve experiments previously described. The p36c12 replicated more quickly than p20c22 in both embryonated eggs and Vero cells.

Subcellular localization of the normal 3b and truncated 3B protein in Cos-7 cells

Finally, the potential influence of the 3b protein on the propagation of virus or its interaction with cellular components was investigated. The normal 3b protein, mutant 3B (C-terminal-truncated) protein, and an N-terminal truncated 3bΔ1 protein were transiently expressed in cells and their subcellular localization patterns were analyzed. For this purpose, a T7-tag (encoding 11 amino acids) sequence was added in frame to the 5′-end of each of the 3b, 3bΔ1, and 3B genes under the control of a T7 promotor. The sequence encoding the first 17 amino acids at the N-terminus of 3b was deleted in the 3bΔ1 construct. The three constructs were confirmed by sequencing and their expressions were analyzed by in vitro transcription and translation (Fig. 7a). The subcellular localization of these proteins was analyzed by indirect immunofluorescent staining at 4, 12, and 24 h posttransfection. The confocal microscopy images of transfected cells were shown in Fig. 7b. At 4 h posttransfection, nuclear localization of the normal 3b and N-terminally truncated 3bΔ1 was observed and these proteins remained exclusively in the nucleus at 24 h posttransfection. In contrast, a defuse distribution pattern was observed for the C-terminal truncated 3B (Fig. 7b). These results indicated that the normal 3b was specifically localized to the nucleus and the C-terminal region of the 3b carried a functional domain related to this nuclear localization. Cos-7 cell, which is also a cell line derived from African green monkey kidney, was used in this experiment because of its higher transfection efficiency compared to Vero cells.

Discussion

We have previously reported that the 3a, 3b, 5a, and 5b proteins of IBV, encoded by sgRNAs 3 and 5, respectively, were expressed in virus-infected cells but were not assembled into virions (Liu et al., 1991a; Liu and Inglis, 1991b, 1992a, 1992b). Little progress has been made since then on the functions of these nonstructural proteins in the life cycle of IBV. Similarly, the functions of nonstructural, accessory proteins encoded by other members of coronaviruses are also unknown, though these proteins are shown to be nonessential for virus propagation in cultured cells and, in some cases, in animal hosts (Luytjes et al., 1988; Schwarz et al., 1990; Weiss et al., 1993; Yokomori and Lai, 1991b; de Haan et al., 2002). In this report, we characterize a mutant with a defective 3b gene encoding a C-terminally truncated product. This was due to a single base insertion at the 5′-terminal portion of the gene, resulting in a novel, frame-shifting product with 17 homogeneous residues at its N-terminus and 17 heterogeneous residues at its C-terminus, instead of 64 residues for the normal 3b protein. The fact that the mutant grows well in cultured cells and in chicken embryos indicates that the 3b gene is nonessential for viral replication.

Interestingly, the mutant emerged and dominated quickly after the prototype strain, EP3, was adapted from the chicken embryo to a monkey kidney cell line. The mutant p36c12 has growth advantage over p20c22 with the normal 3b gene in both Vero cells and chicken embryos and has larger plaque sizes than p20c22. It appears that the mutation in the 3b gene, together with the two mutations in the 195kDa and one in the S protein, renders growth advantages to the mutant and determines its fate in virus evolution: survival or extinction. Clearly, the winner is the one that changes its coding capacity and therefore is fitter than others in a highly competitive, coexisting environment under selective pressures, in this case, continuous passages perhaps at a high multiplicity of infection in a new host.

The growth advantage of p36c22 over p20c22 was also reflected in the different virulence between the two isolates in chicken embryos. P36c12 grew more quickly and caused death of the infected embryos significantly earlier than p20c22. In addition to the single A insertion in the 3b gene, an I^{769}-M^{769} substitution in the S2 region was also observed. However, it was noted that sequencing of the equivalent region of dominant strains from passages 50 and 65 showed that the predicted residue was an Ile at this position instead of a Met, suggesting that the strain with the I^{769}-M^{769} mutation did not dominate in the populations. Furthermore, no difference between S with I^{769} and S with M^{769} in induction of membrane fusion was observed when the two constructs were expressed in Vero cells. At present the mechanism that dictates the growth advantage of the mutant carrying a truncated 3b gene remains unclear. The other two amino acid substitutions in the 195kDa protein might also be involved in the phenotype changes.

The function of the 3b protein in the replication and pathogenesis of IBV is currently unknown. Initial characterization of the protein by fusing the coding sequence of 3b or 3B with a T7-tag sequence showed that the normal 3b protein was able to translocate to the nucleus, whereas the truncated product showed a defuse pattern. The evidence showed that the C-terminal portion of 3b was responsible

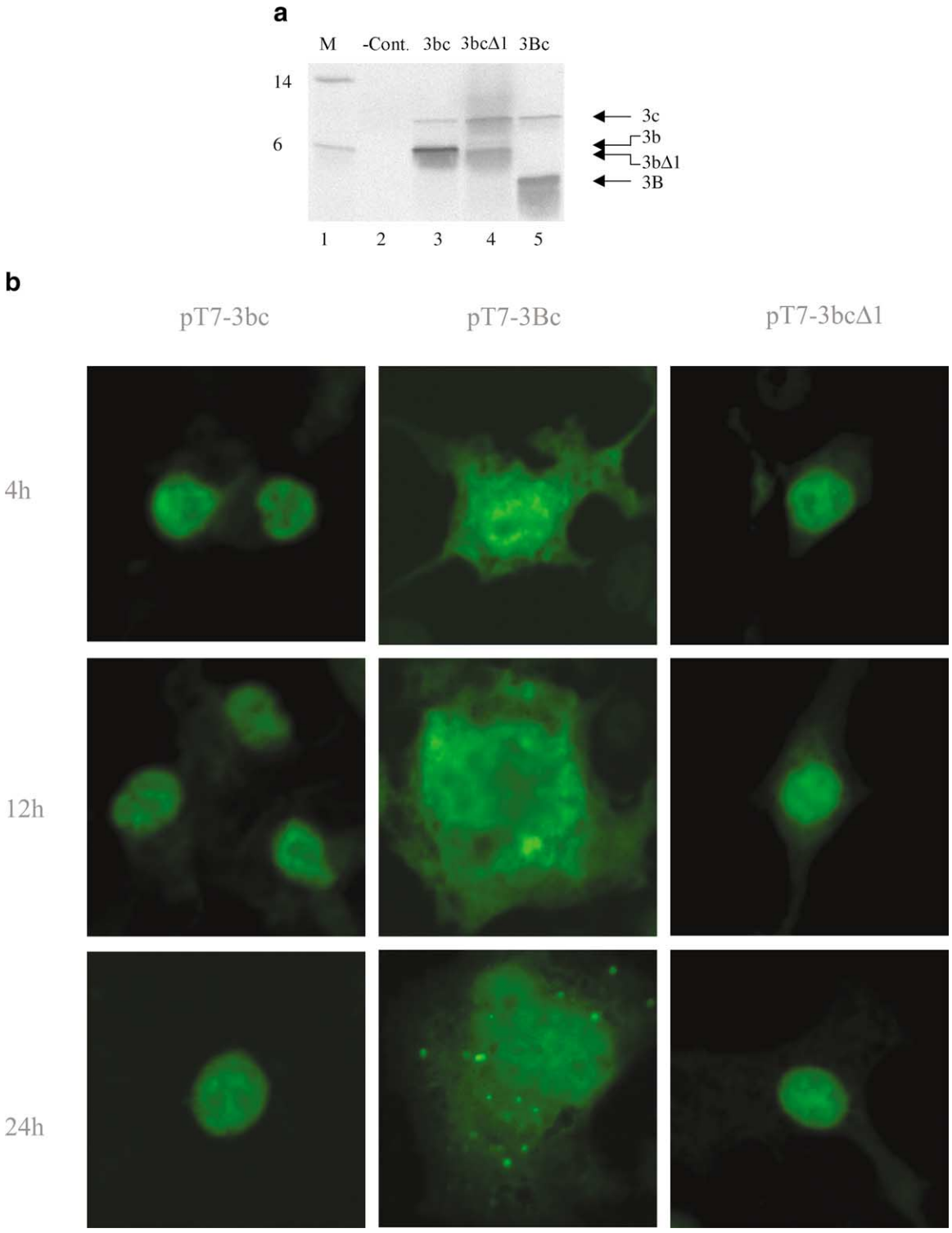

Fig. 7. (a) in vitro translation of constructs containing the T7-tagged, normal 3b, N-terminally truncated 3bcΔ1, and C-terminally truncated 3B gene. Equal amounts of RNA derived from pT7-3bc, pT7-3bcΔ1, and pT7-3Bc were used for in vitro translation in wheat germ lysates. Numbers on the left indicate molecular masses in kilodaltons. (b) Subcellular localization of the normal or truncated 3b proteins transiently expressed in Cos-7 cells. Cells were transfected with indicated plasmid DNA at 1 h postinfection. Cells in chamber slide were stained with anti-T7 monoclonal antibodies and the FITC-conjugated secondary antibodies at different time points. The fluorescence was viewed using a confocal scanning Zeiss microscopy.

for the nuclear localization. In this study, the mechanism by which the IBV 3b protein was localized to the nucleus was not elucidated. Because of the lack of a conventional nuclear-localization signal in the 3b protein, it is likely that the specific localization to the nucleus is due to the interaction of the 3b protein with a host protein. Meanwhile, it would

be interesting to investigate whether the 3b protein may interact with the N protein, which tranlocates to the nucleolus and interacts with nucleolar antigens, fibrillarin, and nucleolin (Wurm et al., 2001; Chen et al., 2002). Further characterization of this localization pattern in IBV-infected cells was hampered by the lack of a highly specific antibody. Nevertheless, as the 3b protein may be the only IBV nonstructural protein that translocates to the nucleus, it is tempting to speculate that the protein might be involved in functions related to the regulation of host functions. Taken together with the observations that the mutant with a truncated 3b gene has growth advantages and is more virulent, the 3b protein might be associated with a cellular antiviral defense system. It has been reported that the nuclear domain 10, a subnuclear structure, is implicated in the modulation of the interferon response (Zheng et al., 1998) and the arenavirus Ring protein targets to this structure, modulating downstream antiviral effects (Borden et al., 1998).

The envelope protein E, together with the M protein, has been proved to play an essential role in the budding of virion in the ER. As the IBV E is encoded by the third ORF of the tricistronic mRNA3 and initiated by ribosome internal entry mechanism (Liu and Inglis, 1992b). The observation that the in vitro expression efficiencies of the E protein encoded by the tricistronic RNAs with or without the single A insertion were at similar levels suggests that the insertion in the 3b did not affect the translation of the E protein. As the ribosome internal entry site (IRES) for the IBV E protein was not well defined, it is unknown if the insertion is in the IRES region. On the other hand, it was observed that p36c12 overgrew p20c22 and was more virulent in chicken embryos than p20c22. As the insertion of an extra A would increase the local AT content, we do not rule out the possibility that this insertion may actually enhance the expression of the E protein in the embryonated eggs.

We are currently exploiting a targeted recombination approach, similar to the one used for MHV (Koetzner et al., 1992; Masters et al., 1994), to investigate which of the mutations, identified in the 195-kDa protein, the S protein, and the 3b protein, plays an essential role in the phenotype changes.

Materials and methods

Cells and viruses

Vero and Cos-7 cells were maintained in DMEM medium (Gibco/BRL, Carlsbad, CA, USA) supplemented with newborn calf serum (10%), streptomycin (1000 μg/ml), and penicillin (1000 units/ml). The Beaudette stain of IBV was purchased from American Type Culture Collection (ATCC) and propagated first in 10-day-old, embryonated eggs for 3 passages. Then the viruses were adapted to grow in Vero cells for 65 passages. Plaque assays were performed as previously described (Shen et al., 1994). P20c22 and p36c12 from passages 20 and 36, respectively, were purified by plaque purification three times. Their genetypes were confirmed by determining the complete genome nucleotide sequence and only the first three passages of each isolate were used. Passage 3 in embryonated eggs and several passages in Vero cells were also used for direct RNA extraction, RT–PCR, and sequence analysis. Recombinant vaccinia/T7 virus (VT3) was grown and titrated on Vero cells.

RT–PCR and sequencing

Viral RNA was extracted from partially purified viruses using the RNeasy mini kit (Qiagen, Chatsworth, CA, USA), according to the manufacturer's instructions. RT–PCR was performed using the Expand Reverse Transcription and High Fidelity PCR kits (Roche). Annealing and extension times were optimized for amplification of PCR products with different sizes using different primers. Specific primers were used for amplification, sequencing, and cloning. Automated sequencing was carried out using PCR products or cDNA clones and specific primers as previously described (Shen et al., 2000). Sequence analysis was carried out using the GCG suite of programs.

Growth curves in Vero cells and embryonated eggs

Vero cells in 35-mm dishes were inoculated with 0.5 ml of virus stock containing 2×10^5 plaque forming units (PFU) (at a m.o.i. of 0.1). After 1 h of absorption, cells were washed once with phosphate-buffered saline (PBS) and incubated at 37°C. One dish from each group infected with p20c22 or p36c12 was removed at each time point and stored at −80°C. For growth curves in chicken embryos, 0.2 ml of each virus containing 4×10^4 PFU was injected into the allantoic cavity of 10-day old, embryonated eggs. The chicken embryos were incubated at 37°C. At each time point, the allantoic fluids from three eggs of each group were collected, centrifuged, and stored at −80°C until the samples were titrated by plaque assays on Vero cells.

Construction of plasmids

RT–PCR fragments were obtained using viral RNAs extracted from p20c22 and p36c12, which contain the normal 3b and mutated 3B genes respectively. Forward primers L52 (AAGTCTGTTCCATGGTCCAAAGTCCC), L53 (CAGTCTAGACCCATGGTAAAC TTAGAAG), and L55 (GATTGTTCAGGCCATGGTGAATTTATTGAA) and the backward primer X7 (CTCTGGATCCAATAACCTA) were designed for three PCR products covering the IBV sequence from nucleotides 23865–24798, 24029–24798, and 24204–24798, respectively. Each PCR product was digested with *Nco*I and *Bam*HI and then ligated into pKT0 (Liu et al., 1994) digested with the same two enzymes, giving rise to pIBV3abc, pIBV3aBc, pIBV3bc, pIBV3Bc, and pIBV3c. Primers L52,

L53, and L55 were designed to contain an *Nco*I site (underlined) flanked with an IBV-specific sequence (20 to 22 nucleotides), whereas X7 was complementary to the IBV sequence from nucleotides 24785–24803 with a *Bam*HI site at 24798. All plasmids described above contain part of the M gene at the 3′-end as well as other gene(s) at the 5′-end of sgRNA 3 as indicated in Fig. 6a.

Plasmids pT7-3bc, pT7-3Bc, and pT7-3bΔ1 were constructed by cloning *Bam*HI-digested RT–PCR fragments into *Bam*HI-cut pT7-tag (Lim and Liu, 2001). The 3b and 3B genes were derived from viral RNAs of p20c22 and p36c12, respectively, and cover the IBV sequence from nucleotides 24033 to 24796. The N-terminally truncated 3bΔ1 gene in pT7-3bΔ1, derived from viral RNA of p20c22, covers the IBV sequence from nucleotides 24084 to 24796. The primers SS2-21 (TAGACGGATCCTAAACTTAGAAGTAATT) and X7 (as indicated above) were used for the PCR amplification of the 3b and 3B genes, and primers SS2-22 (TTCAAAGGATCCGTTTCAATTTACAGCA) and X7 were used for the 3bΔ1 gene. The primers contain the *Bam*HI site (underlined) for cloning. The three genes were fused at the 5′-end with a 33-nucleotide T7-tag and placed under the control of a T7 promoter.

Plasmids pIBV-S20 and pIBV-S36 were obtained by cloning RT–PCR fragments, restricted with *Bam*HI, into *Bgl* II–*Bam*HI-digested pKT0. The two plasmids contain the S gene and cover the IBV sequence from nucleotides 20365–24027, amplified from viral RNA of p20c22 and p36c12, respectively. The primers X9 (GTTACTGGATCCAGATGTTG) and XHY12 (AAGTTGGATCCAGTCTAGACTG TGCC) used contain an IBV-specific sequence and *Bam*HI site (underlined).

Transcription and translation in vitro

Transcription and translation in vitro were performed using T7 RNA polymerase and wheat germ lysates (Promega) as previously described (Shen et al., 1999). in vitro transcription and translation were carried out separately to assess the quantity of transcripts and efficiency of translation of each gene in each construct. The synthesized proteins were radiolabeled with [^{35}S]-methionine. Aliquots of the products were analyzed by 17.5% SDS–PAGE and detected by autoradiography as previously described (Shen et al., 1999).

Membrane fusion experiments

Confluent Vero cells were infected with recombinant vaccinia/T7 viruses at a m.o.i. of 0.1. After 1 h of attachment, cells (2×10^7) were trypsinized, centrifuged at 300*g*, and resuspended in 2 ml of PBS. The cells (0.3 ml) were mixed with 5 μg of plasmid. The mixture was electroporated (Easyject, EquiBio) at 600 V in a 0.4-cm cuvette (Bio-Rad). The cells were then plated in a 35-mm dish containing DMEM with 2% of newborn calf serum and incubated at 37°C.

Analysis of virulence of viruses on embryonated eggs

Ten-day-old chicken embryonated eggs were obtained from a specific-pathogen-free (SPF) farm (Lim Chu Kang Veterinary Station, Singapore) and were used for inoculation with viruses. The titers of virus stocks were determined by plaque assays, and the dosage that could cause the death of 100% of chicken embryos within 2 to 3 days was determined. The difference in virulence was compared between the isolates p20c22 and p36c12 by inoculating no more than 100 PFU per egg and evaluation of the time needed to cause 50% of the death of the infected embryos. The death of the infected embryos was confirmed by examining the embryos that were curled, dwarfed, bleeding, and without body movement.

Immunofluorescence and confocal microscopy

Cells grown on chamber slides (Iwaki) were infected with recombinant vaccinia/T7 viruses. After incubation at 37°C for 1 h, cells were transfected with appropriate plasmid DNA with a T7-tag sequence at the 5′-end of the normal or truncated 3b gene using Dotap Lipisomal Transfection Reagent (Roche). At different time points, cells were fixed in 4% paraformaldehyde–PBS for 15 min and permeabilized with 0.2% Triton X-100–PBS for 10 min. Immunofluorescent staining was performed by incubating cells with anti-T7 monoclonal antibodies (1:200; Novagen) for 1 h and subsequently with FITC-conjugated goat antimouse antibody (1:80; Dako) for 1 h. Both primary and secondary antibodies were diluted in PBS containing 5% goat serum. Cells were rinsed three times with PBS after each step and images were viewed with a Zeiss confocal microscopy and scanned with a connected Bio-Rad MRC1024 scanner.

Acknowledgments

We thank Ms. Dora Chin-Yen Koh and Mr. Li Yu for technique assistance. This work was supported by a grant from the National Science and Technology Board (NSTB), Singapore.

References

Borden, K.L., Campbell Dwyer, E.J., Salvato, M.S., 1998. An arenavirus RING (zinc-binding) protein binds the oncoprotein promyelocyte leukemia protein (PML) and relocates PML nuclear bodies to the cytoplasm. J. Virol. 72, 758–766.

Bos, E.C., Luytjes, W., van der Meulen, H.V., Koerten, H.K., Spaan, W.J., 1996. The production of recombinant infectious DI-particles of a murine coronavirus in the absence of helper virus. Virology 218, 52–60.

Boursnell, M.E., Brown, T.D., Foulds, I.J., Green, P.F., Tomley, F.M., Binns, M.M., 1987. Completion of the sequence of the genome of the coronavirus avian infectious bronchitis virus. J. Gen. Virol. 68, 57–77.

Bredenbeek, P.J., Noten, A.F., Horzinek, M.C., Spaan, W.J., 1990. Identification and stability of a 30-kDa nonstructural protein encoded by mRNA 2 of mouse hepatitis virus in infected cells. Virology 175, 303–306.

Cavanagh, D., Davis, P.J., Darbyshire, J.H., Peters, R.W., 1986. Coronavirus IBV: virus retaining spike glycopolypeptide S2 but not S1 is unable to induce virus-neutralizing or haemagglutination-inhibiting antibody, or induce chicken tracheal protection. J. Gen. Virol. 67 (7), 1435–1442.

Cavanagh, D., Brian, D.A., Brinton, M.A., Eujuanes, L., Homles, K.V., Horzinek, M.C., Lai, M.M.C., Laude, H., Plagemann, P.J.W., Siddell, S.G., Spaan, W., Taguchi, F., Talbot, P.J., 1997. Nidovirales: a new ordor comprising Coronaviridae and Arteriviridae. Arch. Virol. 142, 629–633.

Cavanagh, D., 2001a. A nomenclature for avian coronavirus isolates and the question of species status. Avian Pathol. 30, 109–115.

Cavanagh, D., Mawditt, K., Sharma, M., Drury, S.E., Ainsworth, H.L., Britton, P., Gough, R.E., 2001b. Detection of a coronavirus from turkey poults in Europe genetically related to infectious bronchitis virus of chickens. Avian Pathol. 30, 365–378.

Cavanagh, D., Mawditt, K., Welchman, Dde. B., Britton, P., Gough, R.E., 2002. Coronaviruses from pheasants (*Phasianus colchicus*) are genetically closely related to coronaviruses of domestic fowl (infectious bronchitis virus) and turkeys. Avian Pathol. 31, 81–93.

Chen, H., Wurm, T., Britton, P., Brooks, G., Hiscox, J.A., 2002. Interaction of the coronavirus nucleoprotein with nucleolar antigens and the host cell. J. Virol. 76, 5233–5250.

de Haan, C.A., Masters, P.S., Shen, X., Weiss, S., Rottier, P.J., 2002. The group-specific murine coronavirus genes are not essential, but their deletion, by reverse genetics, is attenuating in the natural host. Virology 296, 177–189.

de Vries, A.A.F., Horzinek, M.C., Rottier, P.J.M., de Groot, R.J., 1997. The genome organization of Nidovirales: similarities and differences between arteri-, toro-, and coronaviruses. Semin. Virology 8, 33–47.

Enjuanes, L., Siddell, S.J., Spaan, W.J., 1998. Coronaviruses and Arteriviruses. Plenum Press, New York.

Enjuanes, L., Brian, D., Cavanagh, D., Holmes, K., Lai, M.M.C., Laude, H., Masters, P., Rottier, P.J.M., Siddell, S.J., Spaan, W.J.M., Taguchi, F., Talbot, P., 2000. Family coronaviridae, in: van Regenmortel, M.H.V., et al. (Eds.), Virus Taxonomy. Academic Press, New York, pp. 835–849.

Fischer, F., Peng, D., Hingley, S.T., Weiss, S.R., Masters, P.S., 1997. The internal open reading frame within the nucleocapsid gene of mouse hepatitis virus encodes a structural protein that is not essential for viral replication. J. Virol. 71, 996–1003.

Guy, J.S., 2000. Turkey coronavirus is more closely related to avian infectious bronchitis virus than mammalian coronaviruses: a review. Avian Pathol. 29, 207–212.

Herrewegh, A.A., Vennema, H., Horzinek, M.C., Rottier, P.J., de Groot, R.J., 1995. The molecular genetics of feline coronaviruses: comparative sequence analysis of the ORF7a/7b transcription unit of different biotypes. Virology 212, 622–631.

Horsburgh, B.C., Brierley, I., Brown, T.D., 1992. Analysis of a 9.6 kb sequence from the 3′ end of canine coronavirus genomic RNA. J. Gen. Virol. 73, 2849–2862.

Koetzner, C.A., Parker, M.M., Ricard, C.S., Sturman, L.S., Masters, P.S., 1992. Repair and mutagenesis of the genome of a deletion mutant of the coronavirus mouse hepatitis virus by targeted RNA recombination. J. Virol. 66, 1841–1848.

Lim, K.P., Ng, L.F., Liu, D.X., 2000. Identification of a novel cleavage activity of the first papain-like proteinase domain encoded by open reading frame 1a of the coronavirus avian infectious bronchitis virus and characterization of the cleavage products. J. Virol. 74, 1674–1685.

Lim, K.P., Liu, D.X., 2001. The missing link in coronavirus assembly. Retention of the avian coronavirus infectious bronchitis virus envelope protein in the pre-Golgi compartments and physical interaction between the envelope and membrane proteins. J. Biol. Chem. 276, 17515–17523.

Liu, D.X., Cavanagh, D., Green, P., Inglis, S.C., 1991a. A polycistronic mRNA specified by the coronavirus infectious bronchitis virus. Virology 184, 531–544.

Liu, D.X., Inglis, S.C., 1991b. Association of the infectious bronchitis virus 3c protein with the virion envelope. Virology 185, 911–917.

Liu, D.X., Inglis, S.C., 1992a. Identification of two new polypeptides encoded by mRNA5 of the coronavirus infectious bronchitis virus. Virology 186, 342–347.

Liu, D.X., Inglis, S.C., 1992b. Internal entry of ribosomes on a tricistronic mRNA encoded by infectious bronchitis virus. J. Virol. 66, 6143–6154.

Liu, D.X., Brierley, I., Tibbles, K.W., Brown, T.D.K., 1994. A 100K polypeptide encoded by open reading frame (ORF) 1b of the coronavirus infectious bronchitis virus is processed by ORF1a products. J. Virol. 68, 5772–5780.

Luytjes, W., Bredenbeek, P.J., Noten, A.F., Horzinek, M.C., Spaan, W.J., 1988. Sequence of mouse hepatitis virus A59 mRNA 2: indications for RNA recombination between coronaviruses and influenza C virus. Virology 166, 415–422.

Masters, P.S., Koetzner, C.A., Kerr, C.A., Heo, Y., 1994. Optimization of targeted RNA recombination and mapping of a novel nucleocapsid gene mutation in the coronavirus mouse hepatitis virus. J. Virol. 68, 328–337.

Ng, L.F., Liu, D.X., 2000. Further characterization of the coronavirus infectious bronchitis virus 3C-like proteinase and determination of a new cleavage. Virology 272, 27–39.

Ontiveros, E., Kuo, L., Masters, P.S., Perlman, S., 2001. Inactivation of expression of gene 4 of mouse hepatitis virus strain JHM does not affect virulence in the murine CNS. Virology 289, 230–238.

Saeki, K., Ohtsuka, N., Taguchi, F., 1997. Identification of spike protein residues of murine coronavirus responsible for receptor-binding activity by use of soluble receptor-resistant mutants. J. Virol. 71, 9024–9031.

Senanayake, S.D., Hofmann, M.A., Maki, J.L., Brian, D.A., 1992. The nucleocapsid protein gene of bovine coronavirus is bicistronic. J. Virol. 66, 5277–5283.

Schwarz, B., Routledge, E., Siddell, S.G., 1990. Murine coronavirus nonstructural protein ns2 is not essential for virus replication in transformed cells. J. Virol. 64, 4784–4791.

Shen, S., Burke, B., Desselberger, U., 1994. Rearrangement of the VP6 gene of a group A rotavirus in combination with a point mutation affecting trimer stability. J. Virol. 68, 1682–1688.

Shen, S., McKee, T.A., Wang, Z.D., Desselberger, U., Liu, D.X., 1999. Sequence analysis and in vitro expression of genes 6 and 11 of an ovine group B rotavirus isolates, Kb63: evidence for a non-defective, C-terminally truncated NSP1 and a phosphorylated NSP5. J. Gen. Virol. 80, 2077–2085.

Shen, S., Kwang, J., Liu, W., Liu, D.X., 2000. Determination of the complete nucleotide sequence of a vaccine strain of porcine reproductive and respiratory syndrome virus and identification of the Nsp2 gene with a unique insertion. Arch. Virol. 145, 871–883.

Taguchi, F., 1995. The S2 subunit of the murine coronavirus spike protein is not involved in receptor binding. J. Virol. 69, 7260–7263.

Thiel, V., Siddell, S.G., 1994. Internal ribosome entry in the coding region of murine hepatitis virus mRNA 5. J. Gen. Virol. 75, 3042–3046.

Vennema, H., Godeke, G.J., Rossen, J.W., Voorhout, W.F., Horzinek, M.C., Opstelten, D.J., Rottier, P.J., 1996. Nucleocapsid-independent assembly of coronavirus-like particles by co-expression of viral envelope protein genes. EMBO J. 15, 2020–2028.

Weiss, S.R., Zoltick, P.W., Leibowitz, J.L., 1993. The ns 4 gene of mouse hepatitis virus (MHV), strain A 59 contains two ORFs and thus differs from ns 4 of the JHM and S strains. Arch. Virol. 129, 301–309.

Wesley, R.D., Woods, R.D., Cheung, A.K., 1990. Genetic basis for the pathogenesis of transmissible gastroenteritis virus. J. Virol. 64, 4761–4766.

Wurm, T., Chen, H., Hodgson, T., Britton, P., Brooks, G., Hiscox, J.A., 2001. Localization to the nucleolus is a common feature of coronavirus nucleoproteins, and the protein may disrupt host cell division. J. Virol. 75, 9345–9356.

Xu, H.Y., Lim, K.P., Shen, S., Liu, D.X., 2001. Further identification and characterization of novel intermediate and mature cleavage products released from the ORF 1b region of the avian coronavirus infectious bronchitis virus 1a/1b polyprotein. Virology 288, 212–222.

Yokomori, K., Banner, L.R., Lai, M.M., 1991a. Heterogeneity of gene expression of the hemagglutinin-esterase (HE) protein of murine coronaviruses. Virology 183, 647–657.

Yokomori, K., Lai, M.M., 1991b. Mouse hepatitis virus S RNA sequence reveals that nonstructural proteins ns4 and ns5a are not essential for murine coronavirus replication. J. Virol. 65, 5605–5608.

Yu, X., Bi, W., Weiss, S.R., Leibowitz, J.L., 1994. Mouse hepatitis virus gene 5b protein is a new virion envelope protein. Virology 202, 1018–1023.

Zheng, P., Guo, Y., Niu, Q., Levy, D.E., Dyck, J.A., Lu, S., Sheiman, L.A., Liu, Y., 1998. Proto-oncogene PML controls genes devoted to MHC class I antigen presentation. Nature 396, 373–376.